ELSEVIER

NeuroImage

www.elsevier.com/locate/ynimg
NeuroImage xx (2004) xxx–xxx

Parametric design and correlational analyses help integrating fMRI and electrophysiological data during face processing

Silvina G. Horovitz,[a,*] Bruno Rossion,[b] Pawel Skudlarski,[c] and John C. Gore[a]

[a] *Institute of Imaging Science, Vanderbilt University, Nashville, TN 37203, USA*
[b] *Unite de Neurosciences Cognitives, Universite Catholique de Louvain, Louvain, la-Neuve, Belgium*
[c] *Department of Diagnostic Radiology—School of Medicine, Yale University, New Haven, CT 06510, USA*

Received 24 November 2003; revised 9 April 2004; accepted 15 April 2004

Face perception is typically associated with activation in the inferior occipital, superior temporal (STG), and fusiform gyri (FG) and with an occipitotemporal electrophysiological component peaking around 170 ms on the scalp, the N170. However, the relationship between the N170 and the multiple face-sensitive activations observed in neuroimaging is unclear. It has been recently shown that the amplitude of the N170 component monotonically decreases as gaussian noise is added to a picture of a face [Jemel et al., 2003]. To help clarify the sources of the N170 without a priori assumptions regarding their number and locations, ERPs and fMRI were recorded in five subjects in the same experiment, in separate sessions. We used a parametric paradigm in which the amplitude of the N170 was modulated by varying the level of noise in a picture, and identified regions where the percent signal change in fMRI correlated with the ERP data. N170 signals were observed for pictures of both cars and faces but were stronger for faces. A monotonic decrease with added noise was observed for the N170 at right hemisphere sites but was less clear on the left and occipital central sites. Correlations between fMRI signal and N170 amplitudes for faces were highly significant ($P < 0.001$) in bilateral fusiform gyrus and superior temporal gyrus. For cars, the strongest correlations were observed in the parahippocampal region and in the STG ($P < 0.005$). Besides contributing to clarify the spatiotemporal course of face processing, this study illustrates how ERP information may be used synergistically in fMRI analyses. Parametric designs may be developed further to provide some timing information on fMRI activity and help identify the generators of ERP signals.

Keywords: Face perception; fMRI; ERP

Introduction

Neuroimaging studies seek to find when and where activation occurs in the brain. Different techniques have different abilities to measure one aspect or the other with adequate resolution. Direct measurements of neuronal electrical activity provide excellent time resolution, in the order of milliseconds, but noninvasive measurements, such as in scalp electroencephalographic (EEG) or magnetoencephalographic (MEG) recordings, have poor spatial resolution. On the other hand, measures that detect activity by indirect hemodynamic effects, such as functional magnetic resonance imaging (fMRI), have excellent spatial resolution, but the ability to detect temporal changes is intrinsically limited by physiological factors that restrict the time resolution to be at best of the order of hundreds of milliseconds (Formisano and Geobel, 2003; Menon and Kim, 1999).

Several approaches have been explored previously to combine these different methods to clarify the spatiotemporal course of information processing. Source localization is one approach commonly applied to identify the sources of activation of event-related potentials (ERPs) or MEG components (Dale and Halgren, 2001; Scherg, 1990). The location of dipoles sources is calculated using the averaged EEG/MEG data and can then be projected onto anatomical MR images (Dale and Halgren, 2001; Dale and Sereno, 1993). However, finding equivalent dipole solutions from ERP or MEG data is an ill-posed problem, even with realistic head models (for constrained approaches, see for example, Miltner et al., 1994; for source localization approaches without constraints, see for example, Pascual-Marqui et al., 1994). Functional MRI data may be used as seeds for the localization algorithms, constraining the sources of ERP components and/or helping to validate the sources found (e.g., Di Russo et al., 2002; Liu et al., 1998, 2002), but many technological and technical issues still prevent the optimal application of integrating fMRI with EEG/MEG source localization (Dale and Halgren, 2001). One of the most important questions is how a physiological event is reflected in different imaging modalities; in particular, when looking at scalp electrical recordings and hemodynamic responses, the question on how a change in the electrical signal is related to the hemodynamic response remains to be answered.

Our approach to integration consists selecting a range of experimental conditions that modify brain activity and identifying those ERP and fMRI responses that vary together and linearly. We measure the amplitude of specific ERP components and use them as regressors for fMRI data to reveal the sites that correlate with the scalp electrophysiological responses. We have previously used this method in an event-related oddball para-

* Corresponding author. Advanced MRI, LFMI, NINDS, NIH 9000 Rockville Pike, Building 10/B1D723, Bethesda, MD 20982. Fax: +1-301-480-1981.
E-mail address: silvina.horovitz@aya.yale.edu (S.G. Horovitz).
Available online on ScienceDirect (www.sciencedirect.com.)

1053-8119/$ - see front matter © 2004 Elsevier Inc. All rights reserved.
doi:10.1016/j.neuroimage.2004.04.018

digm to identify the cerebral regions involved in generating the P300 (Horovitz et al., 2002). In the present study, we applied this method to an earlier ERP component in the visual domain, the occipitotemporal N170. The N170 is a large posterior negative deflection that follows the visual presentation of a picture of a face, peaking at occipitotemporal sites at around 170 ms (Bentin et al., 1996; Bötzel et al., 1995). The N170 peaks around the same latency for faces and other objects (e.g., houses, chairs, cars, or novel objects such as Greebles or 2D "blob" shapes) but is much larger in response to face pictures (Bentin et al., 1996; Bötzel et al., 1995; Eimer, 2000; Rossion et al., 2000, 2003). Similar findings have been made using MEG (e.g., Halgren et al., 2000).

Alternative theoretical interpretations exist for explaining the amplitude differences of N170s between faces and other objects (see Rossion et al., 2002). The precise origins of the N170 component have also been debated. Bentin et al. (1996) speculated that the N170 originates mainly from the medial wall of the occipitotemporal sulcus, not from the adjacent fusiform gyrus, although these authors later acknowledged the possibility of a contributing source also in that region (Sagiv and Bentin, 2001). However, recent studies applied source localization algorithms on the N170 and disclosed dipolar sources in the bilateral posterior part of the fusiform gyrus or inferior occipital cortex (Halgren et al., 2000; Itier and Taylor, 2002; Rossion et al., 2003; Schweinberger et al., 2002; Watanabe et al., 2003), with a right hemisphere advantage in some studies (Halgren et al., 2000; Rossion et al., 2003). This N170 source localization lies somewhat in between two regions of the ventral processing stream where larger responses to faces compared to objects have been found in humans using neuroimaging: the middle fusiform gyrus (Kanwisher et al., 1997; see also Puce et al., 1995; Sergent et al., 1992) and the inferior occipital cortex (e.g., Gauthier et al., 2000; Haxby et al., 2000), with a clear right hemisphere advantage in both cases (Rossion et al., 2000; Sergent et al., 1992). ERPs recorded from subdural electrodes in patients with intractable epilepsy also indicate that face-sensitive activity occurs in bilateral fusiform gyrus at around 200 ms poststimulus (Allison et al., 1999; McCarthy et al., 1999; Puce et al., 1999).

However, the limited spatial resolution of ERPs and the uncertainty associated with source localization modeling do not allow strong conclusions to be drawn as to the exact location of the N170 sources, as this method cannot spatially dissociate among the sources of different object categories (Rossion et al., 2003). Moreover, different designs and methods of analyses are used in the two cases (ERPs and fMRI) making interstudy comparisons uncertain. As a matter of evidence, the areas responsive to faces are defined only functionally, that is, as a result of a subtraction between the processing of faces and objects. In contrast, most source localizations of the face-N170 or MEG components have been made on the raw ERP response to faces (Itier and Taylor, 2002; Schweinberger et al., 2002; Watanabe et al., 2003) rather than on the subtraction wave between faces and objects (but see Halgren et al., 2000; Rossion et al., 2003).

In the present study, we aimed at clarifying the sources of the N170 response using a parametric design in the same subjects during face and object processing in fMRI and ERPs. The parameter manipulation was based on a recent ERP study (Jemel et al., 2003) in which it was shown that the amplitude of the N170, but not of preceding visual components such as the P1, monotonically increases as a face emerges form gaussian noise.

Here, we took advantage of this systematic variation in the amplitude of the N170 to explore the fMRI data, voxel-by-voxel, and define the regions that modulate the N170 component. Our design differed in several aspects from Jemel et al. (2003). First, the order of stimulus presentation was not organized according to the level of noise (from full noise to clear stimuli, see Jemel et al., 2003). Second, we also used a set of control objects—3/4-view car pictures as in several previous ERP studies on the N170 (e.g., Goffaux et al., 2003; Rossion et al., 2003)—that were presented with the same noise degradation.

Methods

Subjects

Five normal volunteers (two males, three females, age ranging from 21 to 35 years) participated in this study. Informed consent was obtained from each subject in accordance with a protocol reviewed and approved by the Human Investigation Committee of Yale University School of Medicine.

Paradigm

Two hundred sixteen pictures were presented in each run. They were faces or cars with different noise levels and different colors. Noisy images were created in Matlab by adding gaussian noise with standard deviation of 0, 0.025, 0.075, 0.1, 0.2, or 5 (σ/N) to each image. The color was grey or magenta (Fig. 1). Pictures were presented for 500 ms every 1.65 s. During the interstimulus interval, a blank screen was presented. Blocks of six of the same object and noise level with different colors pseudorandomly intermixed were presented to obtain a sustained hemodynamic response (Fig. 2). To maintain their attention throughout the whole recording sessions, subjects were asked to respond to the color of the image presented (grey or magenta). Six to eight runs of fMRI and four runs of ERP were collected for each of the five subjects.

EEG data collection

EEG was collected with a Neuroscan system, using a modified cap with 32 tin electrodes and common linked-ear-lobes reference. Impedances were kept below 10 kΩ. A ground electrode was placed on the forehead. Gain was set to 2500, and sample rate to 500 Hz; acquisition bandwidth was between 0.01 and 70 Hz. Data processing was performed using Scan 4.2 software (Neuroscan Inc., El Paso, Texas). First, data were bandpass-filtered (1–30 Hz). Second, ocular artifacts were removed using the method proposed by Semlitsch et al. (1986). Data were then referenced to a common average reference, divided into epochs starting 200 ms previous to the object presentation and lasting for 998 ms after the onset of the stimulus, and the epochs were then baseline-corrected (−200 to 0 ms). Finally, for each subject, an average wave was obtained for each category and noise level. Grand averages were also obtained for display purposes.

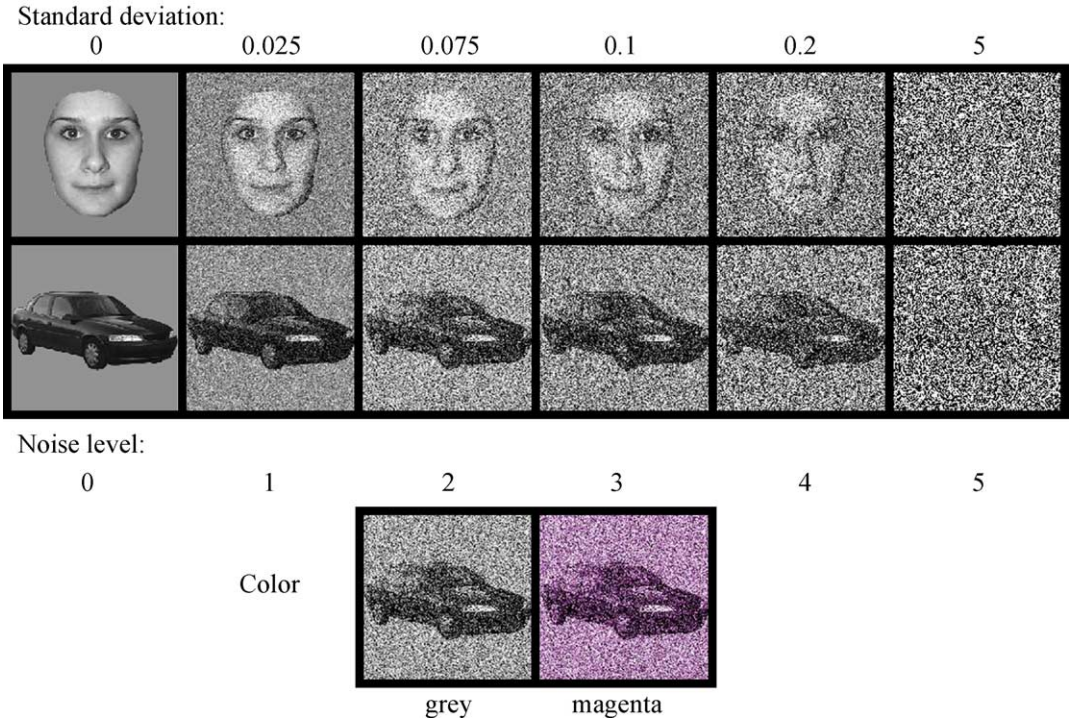

Fig. 1. Examples of stimuli used in the experiment. Gaussian noise was added to the images to obtain six different 'noise levels' ranking from 0 to 5. The corresponding noise levels were obtained via degradation of the image using Gaussian noise of standard deviations of 0, 0.025, 0.075, 0.10, 0.20, or 5. Images were grey or magenta for each noise level.

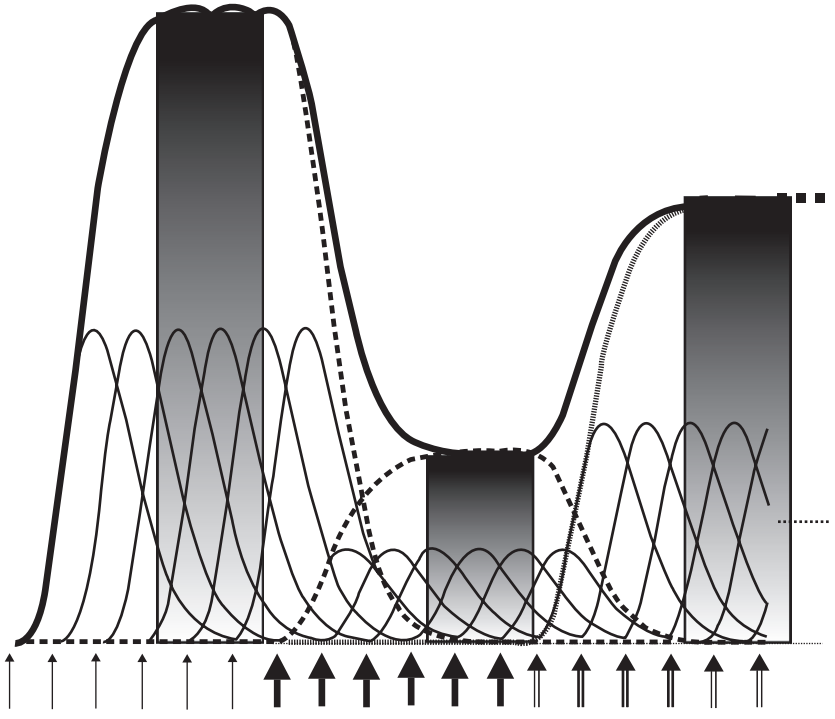

Fig. 2. Simulated time series. Thin lines represent t he responses to individual events; dashed lines indicate the response for each block of six images of the same type and noise level; thick lines represent the overall time course. Bars represent images 4, 5, and 6 of each block; these images are where the hemodynamic responses have reached a steady-state value and are the ones used for the analysis. Arrow thickness indicates the level of noise in the image (in this simulation: low, high, and medium respectively).

EEG data analysis

Peak latency and amplitude values of the N170 were extracted as the maximum (negative) amplitude value between 100 and 200 ms at occipitotemporal electrode sites in the left and right hemispheres. P1 values were measured as the positive peak preceding the N170 wave. Repeated-measures ANOVAs were computed on peak amplitudes and latencies of the N170 and P1 waves measured at locations P8, P7, PO8, PO7, O1, and O2 from the extended standard 10/20 system, see Fig. 3.

fMRI data collection

Images were acquired using a 1.5 T Signa LX scanner (General Electric, Milwaukee, WI). First, T1-weighted images were collected of 18 slices perpendicular to the AC-PC line (identified from a midline-sagittal localizing scan) with a 9-mm slice thickness and a 1-mm interslice gap, getting full head coverage. Functional data were then collected in the same planes, using a single shot gradient echo-planar imaging sequence (TR/TE: 1650/60 ms, flip angle = 60°, FOV = 20 × 20 cm^2, and matrix size = 64 × 64, leading to a voxel size of 3.125 × 3.125 × 9 mm^3).

fMRI data analysis

MRI data were first motion-corrected using SPM99 software [Wellcome Department of Cognitive Neurology, University College, London, (http://www.fil.ion.ucl.ac.uk/spm)]. The remaining analysis, including the calculation of statistical maps, was performed using the Yale fMRI Analysis Package (http://mri.med.yale.edu/individual/pawel/fMRIpackage.html) running under MATLAB (The MathWorks Inc., Natick, MA). Functional images were realigned and registered with the corresponding T1-weighted anatomical images. Pixels with signal smaller than 5% of the maximum value for each run were masked to reduce noise. Images were smoothed in the space domain using a Gaussian filter (6.25 mm FWHM) and high-pass-filtered (0.006 Hz) in the time domain to reduce effects of time drifts (Skudlarski et al., 1999). Data were then converted into Talairach space (Talairach and Tournoux, 1988).

ROI analysis

The midfusiform region was functionally defined for each subject as a result of a statistical map (*t* test) of faces versus cars. Each subject's map was constructed by first collapsing data across noise levels 1, 2, and 3 (see Fig. 1). From these data, the signal at images 4, 5, and 6 after presentation of the first face picture of a block was compared with the signal at images 4, 5, and 6 after presentation of the first picture of the car in a block (see Fig. 2). Once the regions were defined, BOLD signal change values were extracted from these voxels for each of the six noise levels and correlated with N170 amplitudes at electrode PO8.

To evaluate whether the correlations were exclusive to the N170 peak or common to other ERP components typically seen in face paradigms, we performed a post hoc correlation of the standardized amplitude of the peaks measured at 100 ms windows in the range of 0 to 800 ms at electrode PO8 with the fMRI signal change measured in the midfusiform gyrus. ERP data were normalized by subtracting the mean and dividing by standard deviation for each subject.

Voxel-by-voxel correlations

Maps of activations were constructed for each object type and noise level taking the images 4, 5, and 6 of each block (as indicated in Fig. 2) and comparing them with the images 4, 5, and 6 of block level 5 (noise). These maps were used for voxel-by-voxel correlation of the fMRI with the N170 amplitude for each subject and then averaged across subjects.

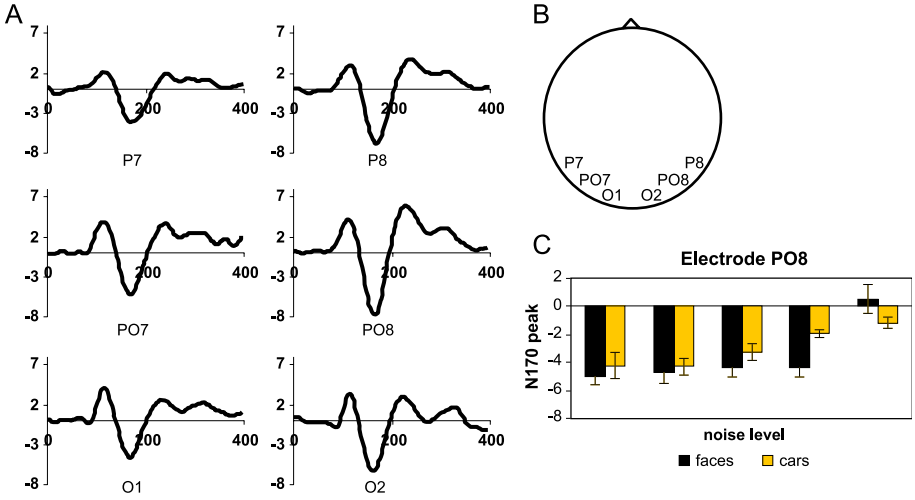

Fig. 3. (A) Grand average of five subjects at noise level 0. Data were low-pass filtered at 15 Hz for presentation. (B) Grand average N170 amplitudes (μV) and standard errors for each noise level and each electrode used for the N170 analysis. (C) Data for 'faces' and 'cars' at electrode PO8. For each subject, the amplitude of the N170 wave at noise 5 was subtracted from the other noise level values; these corrected values were then the used for the group averages. Therefore, the five levels shown are noise levels 0 to 4.

Results

ERP data

N170 waves were observed in all subjects for both cars and faces in all conditions (see Fig. 3); however, N170 amplitudes were larger in response to faces than to cars. The repeated-measures ANOVA model included four factors: Noise level (0–5), Category (face/car), Electrode (P/PO/O), and Hemisphere (right/left). Reported values are Greenhouse-Geisser-corrected.

For the amplitude of the N170 data, main effects were significant for Noise level (P = 0.022), reflecting the decrease of the N170 for higher levels of noise (Fig. 4), and for Category (P = 0.019), reflecting the larger N170 amplitude in response to faces compared to the one for cars. There was no significant interaction between the two factors. The linear contrast was also significant for Noise level (P = 0.007). Latency was significant for electrode (P = 0.012) and side (P = 0.044). P1 amplitude did not significantly differ for any of the variables (Noise level, Category, Electrode, or Hemisphere). Latency was significant for electrode (P = 0.019), and also there was a significant interaction between object and electrode.

ROI analysis for faces

In all subjects, the midfusiform region sensitive to faces was identified in the right hemisphere (mean center of activation: x = 34.7 ± 3.5; y = −53.0 ± 5.3; z = −12.7 ± 4.8). For the correlation between N170 peaks and BOLD signal change in fusiform area, r was −0.728. An example of the fusiform region, the average time course, the ERP data, and the ERP_{N170}−fMRI correlation—displayed as a scatter plot—are shown in Fig. 4.

The post hoc analysis indicated that N170 interval was indeed the interval with the largest correlation; the next highest correlate was the positive peak in the interval 250 to 350 ms (r = −0.555).

Correlations on a voxel-by-voxel basis

Correlations between MRI data and N170 amplitudes for faces at electrode PO8 were most significant (P < 0.001) in bilateral fusiform gyri, in the right middle frontal gyrus, and in the anterior cingulate/top of caudate body (see Fig. 5a and Table 1). Correlations with electrode P7 showed highest significance (P < 0.001) in the right superior temporal gyrus (see Fig. 5b and Table 1). For cars, no significant correlations were

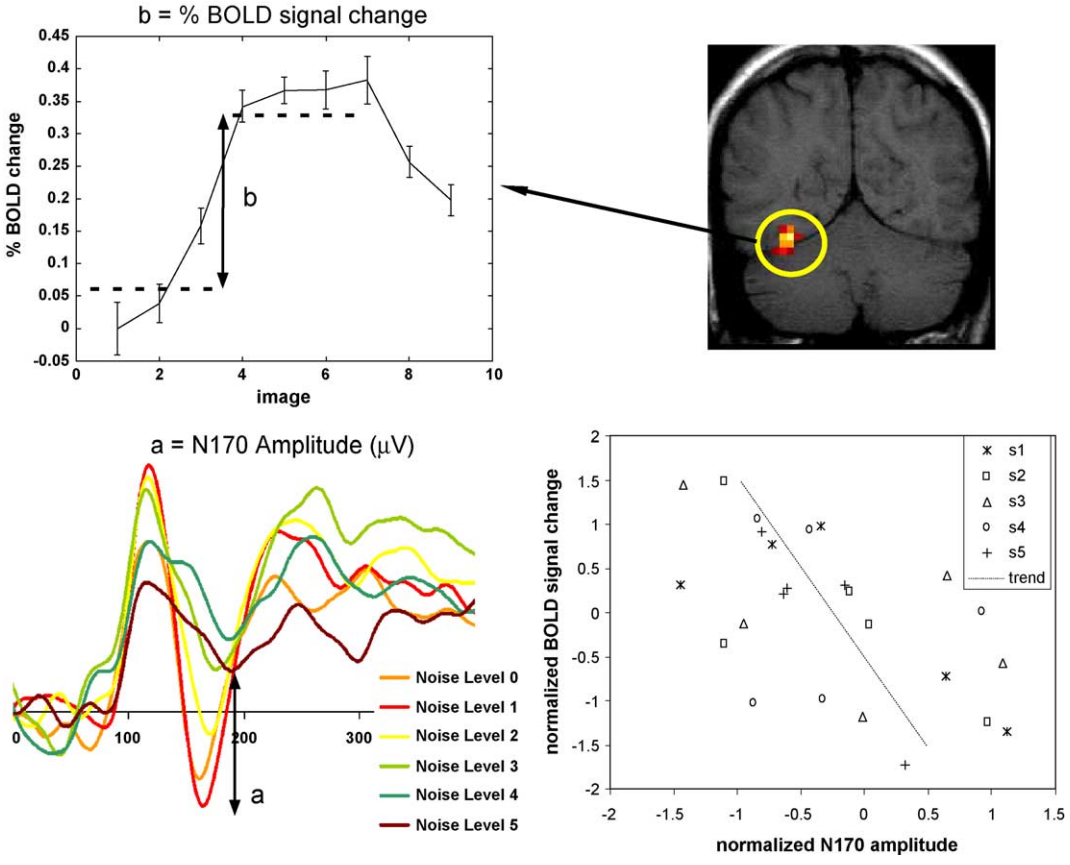

Fig. 4. Correlation between N170 amplitude and midfusiform activation. The region is defined for each subject, and the time course extracted from the region. The % signal change (b) is computed and used to correlate with the N170 amplitude. N170 amplitude is computed by subtracting the amplitude at noise level 5 from the other values (a). The scatter plot shows the data from all subjects and all noise levels for face presentations. It can be observed that the ERP (a) and BOLD % signal change (b) are modified by the experimental manipulation in a linear fashion (r = − 0.728). Data shown correspond to ROI on FFA defined for each subject and amplitude of N170 at electrode PO8.

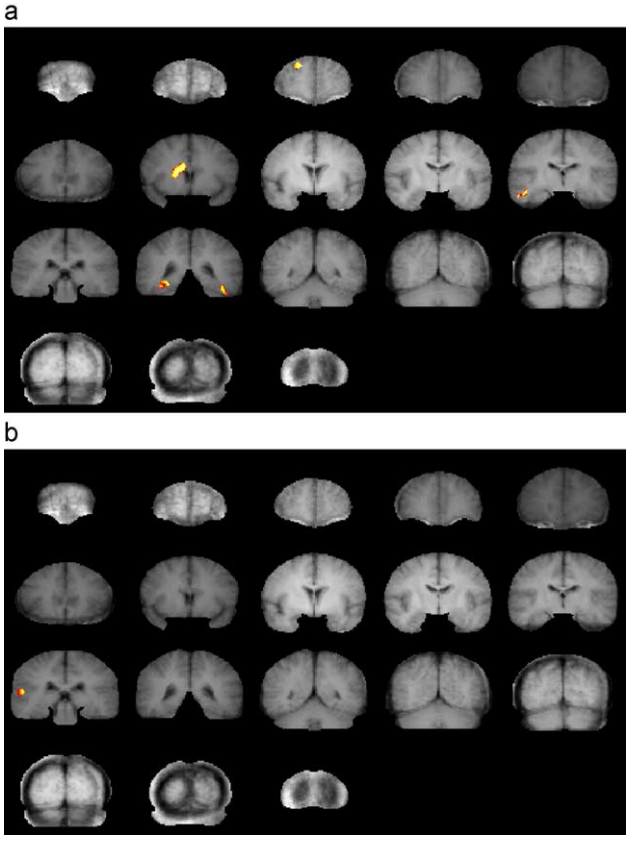

Fig. 5. (a) Activation maps observed for correlations between N170 amplitudes at electrode PO8 and fMRI signal change, results for 'faces' at a threshold value of 0.001 and cluster of 20. Maps are composites of 5 subjects. (b) Activation maps observed for correlations between N170 amplitudes at electrode P7 and fMRI signal change, results for 'faces' at a threshold value of 0.001 and cluster of 20. Maps are composites of five subjects.

observed at the threshold used for faces. When decreasing the threshold to 0.005, significant correlations were observed at left inferior temporal gyrus, parahippocampal gyrus, posterior cingulate, and other regions as indicated in Table 1 for electrode PO8 (also see Fig. 6a), and the strongest correlations between ERP amplitude at electrode P7 and fMRI data were observed in the superior temporal gyrus ($P < 0.001$) (see Fig. 6b and Table 1).

Discussion

Our aim was to show that it is possible to extract some information about the sources of a visual-evoked potential, the N170, without any a priori assumption regarding the number and locations of the sources, using EEG and fMRI data.

Interpretability of the correlations

In principle, the BOLD signal in an area will be sensitive to any change of neural activity that requires an increase of metabolism (associated with an increase of cerebral blood flow and volume, and blood oxygenation). It could thus be directly proportional to both an increase in the number of spikes per second (Rees et al. 2000) and an increase of activity at the postsynaptic (dendritic) level. Field potentials represent slow events—compared to the rate of spikes—reflecting synchronous activity in neural populations, and are thought to represent mostly, but not exclusively, excitatory or inhibitory postsynaptic activity. Thus, in principle, an increase in the rate of spikes, although requiring an increase of metabolism, may not lead to spectacular changes in the LFPs if postsynaptic activity did not increase much or if it was not synchronized among cells forming a population. Conversely, a change in synchrony without a change in the mean activity at the postsynaptic level could lead to LFPs changes without an increase of BOLD. However, current evidence suggests that the BOLD signal measured in fMRI has actually a tighter correlation with local field potentials (LFP) than with multi-unit spiking activity or the rate of single spikes (Logothetis et al., 2001). In most conditions, LFPs are good predictors of the BOLD signal (see Logothetis, 2003). When recording on the scalp, far from the

Table 1
Centers of mass for correlation maps

Object	Electrode	Region	Side	*x*	*y*	*z*	Size	Mean
FACE	PO8	GFm	R	19	40	29	21	0.9998
		Anterior cingulate/ top of caudate	R	15	4	17	57	0.9997
		Fusiform gyrus/ inf. temp. gyrus	R	49	−20	−15	23	0.9995
		Fusiform gyrus	R	31	−40	−6	32	0.9995
		Fusiform gyrus	L	42	−40	−15	22	0.9995
FACE	P7	STG	R	54	−32	14	21	0.9995
CAR	PO8	Inferior frontal gyrus	R	45	24	16	31	0.9971
		Lentiform nucleus	L	14	−4	0	23	−0.9983
		Parahippocampal region/pulvinar	L	31	−32	−1	31	0.9980
		Posterior cingulate	L	12	−50	−5	37	0.9980
		Inferior temporal gyrus	R	52	−70	12	20	0.9978
CAR	P7	STG	R	48	−40	9	43	0.9984
		STG	R	54	4	−1	28	−0.9980

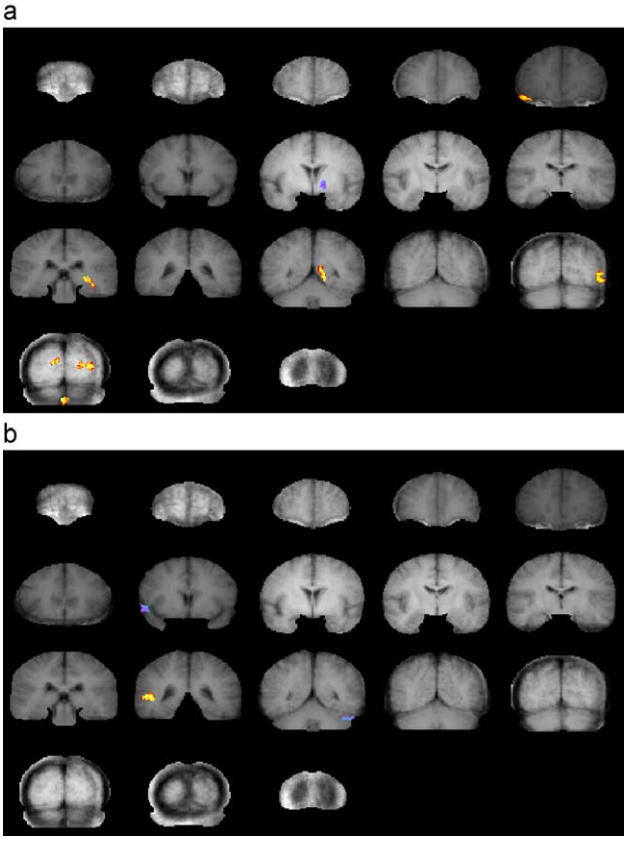

Fig. 6. (a) Activation maps observed for correlations between N170 amplitudes at electrode PO8 and fMRI signal change, results for 'cars' at a threshold value of 0.005 and cluster of 20. Maps are composites of five subjects. (b) Activation maps observed for correlations between N170 amplitudes at electrode P7 and fMRI signal change, results for 'cars' at a threshold value of 0.005 and cluster of 20. Maps are composites of five subjects.

source of field potentials, there are, however, a number of limitations that should be kept in mind. First, depending on the direction of the current flow, the ERP may not be detected on the scalp, since electrodes are located only on the superior part of the head. Second, certain structures such as the amygdala do not have an open field configuration. That is, cells are organized in such a way that they will cancel each other's field and will not be detectable by electrodes placed outside of the structure. This concerns mostly subcortical structures (nuclei). Finally, at least for ERPs, the electrical field recorded on the scalp is distorted by the brain tissue and the skull (which acts as a low-pass filter), and thus activity from deep structures is less visible on the scalp, compared to activities elicited at the cortical surface of the brain.

These possible limitations apply to the different integration approaches including source localization and our correlations using parametric manipulations of a process of interest.

ERP and fMRI correlations

To integrate fMRI and EEG information, we first identified the midfusiform gyrus in response to faces in each subject, as is traditionally done, by subtracting activation for objects from that observed for faces (Kanwisher et al., 1997). We found activations for faces for all subjects within millimeters of the region previously described in the literature (e.g., Gauthier et al., 2000; Kanwisher et al., 1997; Puce et al., 1995) and defined ROIs based on that activation. The mean BOLD signal change of the ROIs for the different noise levels was significantly correlated with the N170 amplitudes at right occipito-temporal electrode PO8 for the same conditions (Fig. 4). This significant correlation indicates that there is a relation between the hemodynamic response in the middle fusiform gyrus and the N170 amplitude.

To verify that the present correlations of the N170 with fusiform BOLD signals were specific to that peak and not related with an overall effect in the ERPs that could artifactually indicate the N170 as origin of the change, we measured the correlations between the BOLD signal change in the middle fusiform gyrus and the ERP amplitudes in electrode PO8, for peaks at 100-ms intervals. The results pointed towards the negative peak at the 100- to 200-ms interval as the strongest correlator with the middle fusiform gyrus. This suggests that the N170 and activity in this region are reflecting related physiological events. Other ERP components showed correlations, but they were much lower.

Although the correlation indicates that the ERP and BOLD signal are affected by the same experimental manipulation, it does not imply that the middle fusiform gyrus is the only source of activation, nor even the main generator of the N170; however, it reinforces the view that this region contributes to the N170 (Itier and Taylor, 2002; Rossion et al., 2003; Schweinberger et al., 2002), since it shows the same functional variations.

More importantly, when data were explored without any prior assumption, the strongest correlations of the N170 amplitude for faces were found for voxels located bilaterally within two standard deviations of the traditionally defined fusiform area (see Table 1).

Our findings and the literature

Taken together, these findings reinforce the view that the sources of the N170 are generated, at least in part, at the middle fusiform gyrus, where face-sensitive responses are observed in humans using neuroimaging (e.g., Gauthier et al., 2000; Haxby et al., 2000; Kanwisher et al., 1997; Puce et al., 1995; Rossion et al., 2000; Sergent et al., 1992) and field potential recordings on the cortical surface (Allison et al., 1999; McCarthy et al., 1999; Puce et al., 1999). These observations are in agreement with source localization of the N170 in EEG and MEG studies (Halgren et al., 2000; Itier and Taylor, 2002; Rossion et al., 2003; Schweinberger et al., 2002; Watanabe et al., 2003), although the localization of the equivalent dipoles is usually found in a slightly more posterior part of the fusiform gyrus. The localization of these face-sensitive regions through correlation with the amplitude of the N170 is also consistent with neuropsychological evidence, showing the involvement of the middle fusiform region in patients presenting face processing deficits (e.g., Barton et al., 2002).

Among the other regions that were identified using the amplitude of the N170 component, the superior temporal gyrus may also be related to the perceptual processing of faces. Face-sensitive responses around this region have been described in several neuroimaging studies in humans (e.g., Hoffman and Haxby, 2000; Kanwisher et al., 1997; Puce et al., 1998). In line

with single-cell recordings in monkeys showing a large proportion of face-selective cells in the lower and upper banks of the superior temporal sulcus (STS; e.g., Hasselmo et al., 1989; Perrett et al., 1985), activation of this region in humans has been related to the perception of the changing aspects of a face, such as expression, eye-gaze, or view (Haxby et al., 2000). Sources located in or around this region and directed towards the lateral part of the cortex may also contribute, together with the fusiform gyrus (Henson et al., 2003; Watanabe et al., 2003), to the N170 scalp potential.

The N170 amplitude was also correlated with differential activity in the anterior cingulate and in the right middle frontal gyrus, two regions that are unlikely to contribute directly to the source of the early visual component on the scalp. The increasing recruitment of these regions with decreasing levels of noise on face stimuli may be associated with differential attentional level and or encoding of high-level visual information in long-term memory. This illustrates an interesting aspect of the method used here, as both direct (i.e., sources) and indirect (i.e., functionally related regions that are not sources) contributions to the electrophysiological responses on the scalp can be disclosed. However, the direct and indirect contributions to scalp ERPs cannot be decoupled objectively using this parametric design and correlation analyses, and complementary source localization analyses would be valuable. In addition, one cannot exclude the possibility that some of the regions presenting correlated variations with the scalp ERP amplitude may be involved at different time scales than when the component is evoked (here between 100 and 200 ms following stimulus onset).

Interestingly, for nonface objects (cars), the strongest correlations between N170 amplitudes and BOLD percentage signal change were observed in the parahippocampal region and in the superior temporal gyrus ($P < 0.005$). Although object categories also appear to recruit a distributed network of regions in the occipitotemporal cortex (Haxby et al., 2001), there is generally a particularly large response to nonface objects in the medial part of the temporal lobe, in or around the region that is most responsive to visual scenes (Epstein and Kanwisher, 1998).

Besides contributing to clarify the spatiotemporal course of face processing, this study illustrates how ERP information may be used synergistically in fMRI analyses. Parametric designs of this type may provide some timing information on fMRI activity and help identify the generators of ERP signals. It has been shown here and in our previous work (Horovitz et al., 2002) that fMRI and ERP parametric studies, when combined with correlation analysis, allow for detection of a more specific network of activations than conventional subtraction methods used in neuroimaging. Yet here, correlations of MRI signals with corresponding ERP data allowed identification of brain areas that agreed well with such conventional subtraction methods. A critical issue for future work in this field is how well the parameter selected affects the response and how specific the effect is across subjects.

Acknowledgments

This project was partially supported by NIH/NIBIB EB-0046102. Bruno Rossion is supported by the Belgian National Fund for National Research (FNRS).

References

Allison, T., Puce, A., Spencer, D.D., McCarthy, G., 1999. Electrophysiological studies of human face perception: potentials generated in occipitotemporal cortex by face and nonface stimuli. Cereb. Cortex 9, 415–430.

Barton, J.J.S., Press, D.Z., Keenan, J.P., O'Connor, M., 2002. Lesions of the fusiform, face area impair perception of facial configuration in prosopagnosia. Neurology 58, 71–78.

Bentin, S., Allison, T., Puce, A., Perez, E., McCarthy, G., 1996. Electrophysiological studies of face perception in humans. J. Cogn. Neurosci. 8, 551–565.

Bötzel, K., Schulze, S., Stodieck, S.R.G., 1995. Scalp topography and analysis of intracranial sources of face-evoked potentials. Exp. Brain Res. 104, 134–143.

Dale, A.M., Halgren, E., 2001. Spatiotemporal mapping of brain activity by integration of multiple modalities. Curr. Opin. Neurobiol. 11, 202–208.

Dale, A.M., Sereno, M., 1993. Improved localization of cortical activity combining EEG and MEG with MRI cortical surface reconstruction: a linear approach. J. Cogn. Neurosci. 5, 162–176.

Di Russo, F., Martinez, A., Sereno, M.I., Pitzalis, S., Hillyard, S.A., 2002. Cortical sources of the early components of the visual evoked potential. Hum. Brain Mapp. 15 (2), 95–111.

Eimer, M., 2000. The face-specific N170 component reflects late stages in the structural encoding of faces. NeuroReport 11, 2319–2324.

Epstein, R., Kanwisher, N., 1998. A cortical representation of the local visual environment. Nature 392, 598–601.

Formisano, E., Goebel, R., 2003. Tracking cognitive processes with functional MRI mental chronometry. Curr. Opin. Neurobiol. 13, 174–181.

Gauthier, I., Tarr, M.J., Moylan, J., Skudlarski, P., Gore, J.C., Anderson, A.W., 2000. The fusiform "face area" is part of a network that processes faces at the individual level. J. Cogn. Neurosci. 12, 495–504.

Goffaux, V., Gauthier, I., Rossion, B., 2003. Spatial scale contribution to early visual differences between face and object processing. Cogn. Brain Res. 16, 416–424.

Halgren, E., Raij, T., Marinkovic, K., Jousmaki, V., Hari, R., 2000. Cognitive response profile of the human fusiform face area as determined by MEG. Cereb. Cortex 10, 69–81.

Hasselmo, M.E., Rolls, E.T., Baylis, G.C., 1989. The role of expression and identity in the face-selective responses of neurons in the temporal visual cortex of the monkey. Behav. Brain Res. 32, 203–218.

Haxby, J.V., Hoffman, E.A., Gobbini, M.I., 2000. The distributed human neural system for face perception. Trends Cogn. Sci. 4, 223–233.

Haxby, J.V., Gobbini, M.I., Furey, M.L., Ishai, A., Schouten, J.L., Pietrini, P., 2001. Distributed and overlapping representations of faces and objects in ventral temporal cortex. Science 293, 2425–2430.

Henson, R.N., Goshen-Gottstein, Y., Ganel, T., Otten, L.J., Quayle, A., Rugg, M.D., 2003. Electrophysiological and haemodynamic correlates of face perception, recognition and priming. Cereb. Cortex 13 (7), 793–805.

Hoffman, E., Haxby, J.V., 2000. Distinct representation of eye gaze and identity in the distributed human neural system for face perception. Nat. Neurosci. 3, 80–84.

Horovitz, S.G., Skudlarski, P., Gore, J.C., 2002. Correlations and dissociations between BOLD signal and P300 amplitude in an auditory oddball task: a parametric approach to combining fMRI and ERP. Magn. Reson. Imaging 20 (4), 319–325.

Itier, R.J., Taylor, M.J., 2002. Inversion and contrast polarity reversal affect both encoding and recognition processes of unfamiliar faces: a repetition study using ERPs. NeuroImage 15, 353–372.

Jemel, B., Schuller, A.M., Cheref-Khan, Y., Goffaux, V., Crommelinck, M., Bruyer, R., 2003. Stepwise emergence of the face-sensitive N170 event-related potential component. NeuroReport 14 (16), 2035–2039.

Kanwisher, N., McDermott, J., Chun, M.-M., 1997. The fusiform face area: a module in human extrastriate cortex specialized for face perception. J. Neurosci. 17, 4302–4311.

Liu, A.K., Belliveau, J.W., Dale, A.M., 1998. Spatiotemporal imaging of human brain activity using functional MRI constrained magnetoencephalography data: Monte Carlo simulations. Proc. Natl. Acad. Sci. U. S. A. 95 (15), 8945–8950.

Liu, A.K., Dale, A.M., Belliveau, J.W., 2002. Monte Carlo simulation studies of EEG and MEG localization accuracy. Hum. Brain Mapp. 16, 47–62.

Logothetis, N.K., 2003. The underpinnings of the BOLD functional magnetic resonance imaging signal. J. Neurosci. 23 (10), 3963–3971 (May 15).

Logothetis, N.K., Pauls, J., Augath, M., Trinath, T., Oeltermann, A., 2001. Neurophysiological investigation of the basis of the fMRI signal. Nature 412 (6843), 150–157.

McCarthy, G., Puce, A., Belger, A., Allison, T., 1999. Electrophysiological studies of human face perception. II: Response properties of face specific potentials generated in occipitotemporal cortex. Cereb. Cortex 9, 431–444.

Menon, R.S., Kim, S.G., 1999. Spatial and temporal limits in cognitive neuroimaging with fMRI. Trends Cogn. Sci. 3, 207–216.

Miltner, W., Braun, C. , Johnson Jr., R., Simpson, G.V., Ruchkin, D.S. 1994. A test of brain electrical source analysis (BESA): a simulation study. Electroencephalogr. Clin. Neurophysiol. 91 (4), 295–310.

Pascual-Marqui, R.D., Michel, C.M., Lehmann, D., 1994. Low resolution electromagnetic tomography: a new method for localizing electrical activity in the brain. Int. J. Psychophysiol. 18 (1), 49–65.

Perrett, D.I., Smith, P., Potter, D.D., Mistlin, A.J., Head, A.S., Milner, A.D., Jeeves, M.A., 1985. Visual cells in the temporal cortex sensitive to face view and gaze direction. Proc. R. Soc. Lond., B 223 (1232), 293–317.

Puce, A., Allison, T., Gore, J.C., McCarthy, G., 1995. Face-sensitive regions in human extrastriate cortex studied by functional MRI. J. Neurophysiol. 74, 1192–1199.

Puce, A., Allison, T., Bentin, S., Gore, J.C., McCarthy, G., 1998. Temporal cortex activation in humans viewing eye and mouth movements. J. Neurosci. 18, 2188–2199.

Puce, A., Allison, T., McCarthy, G., 1999. Electrophysiological studies of human face perception. III. Effects of top-down processing on face-specific potentials. Cereb. Cortex 9, 445–458.

Rees, G., Friston, K., Koch, C., 2000. A direct quantitative relationship between the functional properties of human and macaque V5. Nat. Neurosci. 3 (7), 716–723.

Rossion, B., Gauthier, I., Tarr, M.J., Despland, P.A., Bruyer, R., Linotte, S., Crommelinck, M., 2000. The N170 occipito-temporal component is enhanced and delayed to inverted faces but not to inverted objects: an electrophysiological account of face-specific processes in the human brain. NeuroReport 11, 69–74.

Rossion, B., Curran, T., Gauthier, I., 2002. A defense of the subordinate-expertise account for the N170 component. Cognition 85, 189–196.

Rossion, B., Joyce, C., Cottrell, G., Tarr, M.J., 2003. Early lateralization and orientation tuning for face, word and object processing in the visual cortex. NeuroImage 20 (3), 1609–1624.

Sagiv, N., Bentin, S., 2001. Structural encoding of human and schematic faces: holistic and part-based processes. J. Cogn. Neurosci. 13, 937–951.

Scherg, M., 1990. Fundamentals of dipole source potential analysis. In: Grandori, F., Hoke, M., Romani, G.L. (Eds.), Auditory Evoked Magnetic and Magnetic and Electric Potentials. Adv. Audiol. Karger, Basel, pp. 40–69.

Schweinberger, S.R., Pickering, E.C., Jentzsch, I., Burton, A.M., Kaufmann, J.M., 2002. Event-related brain potential evidence for a response of inferior temporal cortex to familiar face repetitions. Cogn. Brain Res. 14, 398–409.

Semlitsch, H.V., Anderer, P., Schuster, P., Presslich, O., 1986. A solution for reliable and valid reduction of ocular artifacts, applied to the P300 ERP. Psychophysiology 23 (6), 695–703.

Sergent, J., Otha, S., MacDonald, B., 1992. Functional neuroanatomy of face and object processing. A positron emission tomography study. Brain 115, 15–36.

Skudlarski, P., Constable, R.T., Gore, J.C., 1999. ROC analysis of statistical methods used in functional MRI: individual subjects. NeuroImage 9 (3), 311–329.

Talairach, J., Tournoux, P., 1988. Co-Planar Stereotaxic Atlas of the Human Brain. 3-Dimensional Proportional System: An Approach to Cerebral Imaging Georg Thieme Verlag, New York, NY.

Watanabe, S., Kakigi, R., Puce, A., 2003. The spatio-temporal dynamics of the face inversion effect: a magneto- and electro-encephalographic study. Neuroscience 116, 879–895.